The electromagnetic form factors and spin polarization of Λ_c^+ in the process $e^+e^- \to \Lambda_c^+ \bar{\Lambda}_c^-$ *

Cheng Chen (陈诚)[1,2†]   Bing Yan (闫冰)[1‡]   Ju-Jun Xie (谢聚军)[1,2,3§]

[1]Institute of Modern Physics, Chinese Academy of Sciences, Lanzhou 730000, China
[2]School of Nuclear Sciences and Technology, University of Chinese Academy of Sciences, Beijing 101408, China
[3]Southern Center for Nuclear-Science Theory (SCNT), Institute of Modern Physics, Chinese Academy of Sciences, Huizhou 516000, China

Abstract: The total cross sections of the process $e^+e^- \to \Lambda_c^+ \bar{\Lambda}_c^-$ close to the threshold are calculated within the vector meson dominance model. It is found that the theoretical results can describe the current experimental measurements. The nontrivial near-threshold energy dependence of the total cross sections of the process $e^+e^- \to \Lambda_c^+ \bar{\Lambda}_c^-$ can be well reproduced by considering the contributions from charmonium-like states and the Coulomb factor. In particular, the results for the angular distribution parameters about the differential cross section are consistent with the experiments from the BESIII Collaboration. In addition, the relative phase $\Delta\Phi$ of the electromagnetic form factors is given, and the spin polarization of Λ_c^+ is predicted at center-mass energy 4.7 GeV. It is hopeful that this work will provide a new perspective on the characteristics of the charmed baryon Λ_c^+.

Keywords: electromagnetic form factors, charmed baryon, spin polarization

I. INTRODUCTION

Electromagnetic form factors (EMFFs) are essential to understanding the electromagnetic structure of baryons [1−3]. In the single photon exchange approximation, the EMFFs are as a function of q^2, and the physical region is categorized into the space-like region ($q^2 < 0$) and time-like region ($q^2 > 0$), according to the transferred four-momentum squared q^2 of the exchanged virtual photon. In the space-like region, the EMFFs are measured by the scattering channel $e^-B \to e^-B$ (B stands for a baryon) [4−6], and reflect the electromagnetic spatial distribution of baryons. However, because of the difficulties in producing stable and high-quality hyperon beams, it is challenging to study the EMFFs of hyperons in the space-like region. In the time-like region, the EMFFs are investigated in the annihilation process $e^-e^+ \to B\bar{B}$ ($\bar{B}$ stands for an antibaryon), which is the main process for studying the EMFFs of unstable baryons [7−14]. Moreover, the EMFFs in the time-like region were considered as the time evolution of the charge and magnetic distributions

inside the baryon [15]. On the other hand, the spin polarization and asymmetry parameters of Λ, Σ, and Ξ hyperons are also measured in the $e^+e^- \to \Lambda\bar{\Lambda}$ [16, 17], $e^+e^- \to \Sigma\bar{\Sigma}$ [14, 18], and $e^+e^- \to \Xi\bar{\Xi}$ [19−21] reactions, respectively. The spin polarization of hyperons is related to the relative phase between their electric G_E and magnetic G_M form factors.

The Λ_c^+ is the lightest baryon with a single-charm quark, and its quantum number spin-parity is $J^P = 1/2^+$. It has only weak decay modes. In 2008, the cross section of the reaction $e^+e^- \to \Lambda_c^+ \bar{\Lambda}_c^-$ was first measured by Belle Collaboration [22]. The corresponding cross section demonstrates a nontrivial energy dependence in the vicinity of the reaction threshold, which shows a resonance structure around 4.63 GeV. In 2018, BESIII Collaboration reported more precise data near the reaction threshold and found the threshold enhancement effect in the process $e^+e^- \to \Lambda_c^+ \bar{\Lambda}_c^-$ [23]. However, the BESIII measurement of the $e^+e^- \to \Lambda_c^+ \bar{\Lambda}_c^-$ reaction from the threshold to 4.6 GeV implies a different energy-dependence trend of the total cross sections [23]. Recently, high-

precision data for the reaction was measured by BESIII Collaboration [24], where the flat cross sections around 4.63 GeV are obtained and no indication of the resonant structure about $Y(4630)$, as reported by the Belle Collaboration [22]. In addition to the total cross section of $e^+e^- \to \Lambda_c^+\bar{\Lambda}_c^-$ reaction, the magnetic form factor $|G_M|$, the ratio $|G_E/G_M|$, and the angular distribution parameter α of Λ_c^+ were also measured in Ref. [24]. In particular, it was found that the energy dependence of the ratio $|G_E/G_M|$ for the Λ_c^+ baryon reveals an oscillation feature.

Before the new measurements of the $e^+e^- \to \Lambda_c^+\bar{\Lambda}_c^-$ reaction by the BESIII Collaboration [24], the final state interactions of the $\Lambda_c^+\bar{\Lambda}_c^-$ pair and the possible $X(4660)$ state were considered in the theoretical studies on the reaction of $e^+e^- \to \Lambda_c^+\bar{\Lambda}_c^-$ [25−27], and the near-threshold enhancement observed by the Belle Collaboration was reproduced. It was noted that a virtual state lying below but very close to the $\Lambda_c^+\bar{\Lambda}_c^-$ mass threshold, located at 4.566 ± 0.007 GeV, caused the threshold enhancement [26]. Moreover, based on the Belle data [22] and the BESIII data [23], both the time-like and space-like EMFFs of the Λ_c^+ were investigated by the vector meson dominance model (VMD) in Ref. [28], in which six charmonium states below the $\Lambda_c^+\bar{\Lambda}_c^-$ mass threshold were included in the model. The new results of Ref. [24] indicate that there are more complicated reaction dynamics behind in the process of $e^+e^- \to \Lambda_c^+\bar{\Lambda}_c^-$. Therefore, further studies on this reaction are needed.

With the new measurements by the BESIII Collaboration [24], in Ref. [29], it is pointed out that the contact potential in the final state $\Lambda_c^+\bar{\Lambda}_c^-$ rescattering plays an important role in the enhancement near the threshold. Up to 4.75 GeV, the available data on the total cross sections of $e^+e^- \to \Lambda_c^+\bar{\Lambda}_c^-$, modulus of the individual EMFFs of Λ_c^+, and their ratio can be well described [29]. Additionally, in Ref. [30], with the VMD model as in Ref. [28], the $e^+e^- \to \Lambda_c^+\bar{\Lambda}_c^-$ cross sections and the time-like EMFFs of Λ_c^+ were investigated by including four charmonium-like states that have been experimentally discovered in recent years [31, 32], called $\psi(4500)$, $\psi(4660)$, $\psi(4790)$, and $\psi(4900)$. It was found that these charmonium-like states are crucial to the nonmonotonic structures of the Λ_c^+ EMFFs and enhancement near the reaction threshold [30]. Especially, the so-called oscillation behavior of the ratio $|G_E/G_M|$ for the Λ_c^+ baryon discovered by the BESIII Collaboration [24] can also be well reproduced. This gives a natural production mechanism for the $e^+e^- \to \Lambda_c^+\bar{\Lambda}_c^-$ reaction.

Here, in this work, motivated by the planed new measurements [33, 34] for the $e^+e^- \to \Lambda_c^+\bar{\Lambda}_c^-$ reaction at threshold, [1] we will focus on the details of electromagnetic form factors of Λ_c^+ based on our previous study [30], including the total cross section near the threshold

and modulus of electric form factor G_E. We will also study the angular distribution parameter α, the relative phase $\Delta\Phi$ between the electric form factor G_E and magnetic form factor G_M, and the spin polarization of Λ_c^+ in the reaction of $e^+e^- \to \Lambda_c^+\bar{\Lambda}_c^-$.

The paper is organized as follows. In the next section, we give the definition of electromagnetic form factors in the reaction of electron-positron annihilation into a baryon and antibaryon pair, and from this, we show the associated spin polarization of the produced charmed baryon Λ_c^+ in the $e^+e^- \to \Lambda_c^+\bar{\Lambda}_c^-$ reaction in Sec. III. Then, we show the theoretical results and discussions in Sec. IV. Finally, a short summary is given in the last section.

II. ELECTROMAGNETIC FORM FACTORS

Generally, the scattering amplitude of the reaction $e^+e^- \to \gamma^* \to B\bar{B}$ (B stands for a baryon with spin-parity $J^P = 1/2^+$) within the one photon exchange approximation can be written as

$$\mathcal{A} = \frac{e^2}{q^2}\bar{v}_e(k_1)\gamma^\mu u_e(k_2)\langle B(p_1)\bar{B}(p_2)|J_\mu^{em}|0\rangle, \quad (1)$$

where $q = k_1 + k_2 = p_1 + p_2$, and the matrix element $\langle B(p_1)\bar{B}(p_2)|J_\mu^{em}|0\rangle$, for the electromagnetic current conservation and Lorentz invariance, could be parameterized by two independent form factors,

$$\langle B(p_1)\bar{B}(p_2)|J_\mu^{em}|0\rangle$$
$$= \bar{u}_B(p_1)\left[F_1(q^2)\gamma_\mu + i\frac{F_2(q^2)}{2M}\sigma_{\mu\nu}q^\nu\right]v_{\bar{B}}(p_2), \quad (2)$$

where M is the mass of baryon B, and $F_1(q^2)$ and $F_2(q^2)$ are the so-called Dirac and Pauli form factors, respectively, with the normalizations $F_1(0) = Q_B$, $F_2(0) = \kappa_B$. Here, Q_B and κ_B denote the charge and anomalous magnetic moment of baryon B. In this way, the electromagnetic information of baryon B is absorbed into the two scalar functions $F_1(q^2)$ and $F_2(q^2)$.

Based on the above formula, the differential cross section of the reaction in the center of mass frame is

$$\frac{d\sigma}{d\Omega} = \frac{\alpha_{em}^2\beta C}{4s} \times \left[|G_M|^2(1+\cos^2\theta) + \frac{4M^2}{s}|G_E|^2\sin^2\theta\right], \quad (3)$$

where $s = q^2$ is the invariant mass squared of the e^+e^- system, and θ is the scattering angle between the momentum of the initial electron and the final baryon B. $\alpha_{em} = e^2/4\pi$ is the electromagnetic fine structure constant, and $\beta = \sqrt{1 - 4M^2/s}$ is the velocity of baryon B. In general, factor C is the S-wave Sommerfeld–Gamow factor

---

1) This is because the Λ_c^+ can be reconstructed via the Cabibbo-favored weak decay of $\Lambda_c^+ \to pK^-\pi^+$, even it was produced at rest.

corresponding to the final state Coulomb interaction of charged baryons [35], which will lead to an unvanished cross section at the threshold, $C = y/(1 - e^{-y})$, $y = 2\pi\alpha_{em}M/(\beta\sqrt{s})$. $C \equiv 1$ for neutral baryons. Considering factor C, it is expected that the cross section of the $e^+e^- \to B\bar{B}$ reaction is nonzero at the reaction threshold for the charged baryon-antibaryon pair of $B\bar{B}$. In addition, G_E and G_M are the electric and magnetic form factors, respectively, which is the linear combination of F_1 and F_2,

$$G_E(q^2) = F_1(q^2) + \tau F_2(q^2), \tag{4}$$

$$G_M(q^2) = F_1(q^2) + F_2(q^2), \tag{5}$$

where $\tau = q^2/4M^2$. At the reaction threshold, $\tau = 1$, thus $G_E = G_M = F_1 + F_2$.

On the other hand, the differential cross section, shown in Eq. (3), can be also expressed in a more compact form

$$\frac{d\sigma}{d\Omega} = N(1 + \alpha\cos^2\theta), \tag{6}$$

with

$$N = \frac{\alpha_{em}^2\beta C}{4s}\left(|G_M|^2 + \frac{4M^2}{s}|G_E|^2\right), \tag{7}$$

$$\alpha = \frac{s|G_M|^2 - 4M^2|G_E|^2}{s|G_M|^2 + 4M^2|G_E|^2}, \tag{8}$$

with α depending on the ratio of the absolute values of the electric and magnetic form factors and satisfying $-1 \le \alpha \le 1$. According to Eq. (6), one can see that the angular distribution of the differential cross section is only dependent on the parameter α. On the theoretical side, once we get the electromagnetic form factors G_E and G_M, we can easily obtain the parameter α from Eq. (8).

Within the above ingredients, and after integrating over the solid angle Ω, the total cross section of the $e^+e^- \to \Lambda_c^+\bar{\Lambda}_c^-$ reaction is obtained as

$$\sigma = \frac{4\pi\alpha_{em}^2\beta C}{3s}\left(|G_M(q^2)|^2 + \frac{2M_{\Lambda_c^+}^2}{s}|G_E(q^2)|^2\right). \tag{9}$$

Note that, on the experimental side, by combining the angular distributions and the total cross sections, the modulus of G_E and G_M for Λ_c^+ could be extracted. [1]

Because of the nonperturbative nature of quantum chromodynamics (QCD) theory in the energy regime of hadrons, an exact theoretical description of their internal structure has not been achieved within the framework of QCD. On the theoretical side, within the extended vector meson dominance model, the Dirac and Pauli form factors $F_1(s)$ and $F_2(s)$ can be phenomenologically parametrized as (more details can be found in Ref. [30]),

$$F_1(s) = \frac{1}{(1 - \gamma s)^2}\left(f_1 + \sum_{i=1}^{4}\beta_i B_{R_i}\right), \tag{10}$$

$$F_2(s) = \frac{1}{(1 - \gamma s)^2}\left(f_2 B_{R_1} + \sum_{i=2}^{4}\alpha_i B_{R_i}\right), \tag{11}$$

with parameter $\gamma = 0.147 \pm 0.017$ GeV^{-2} and

$$B_{R_i} = \frac{M_{R_i}^2}{M_{R_i}^2 - s - iM_{R_i}\Gamma_{R_i}}, \tag{12}$$

where we take $R_1 \equiv \psi(4500)$ with mass $M_{R_1} = 4500$ MeV, $R_2 \equiv \psi(4660)$ with mass $M_{R_2} = 4670$ MeV, and width $\Gamma_{R_2} = 115$ MeV [36]; $R_3 \equiv \psi(4790)$ with $M_{R_3} = 4790$ MeV and $\Gamma_{R_3} = 100$ MeV [32]; $R_4 \equiv \psi(4900)$ with $M_{R_4} = 4900$ MeV and $\Gamma_{R_4} = 100$ MeV [37−39]. Note that because the mass of $\psi(4500)$ is below the $\Lambda_c^+\bar{\Lambda}_c^-$ threshold, for its width we take the Flatté type [40]

$$\Gamma_{\psi(4500)} = \Gamma_0 + g_{\Lambda_c}\sqrt{\frac{s}{4} - M_{\Lambda_c^+}^2}, \tag{13}$$

with $\Gamma_0 = 125$ MeV [31] and the coupling $g_{\Lambda_c} = 1.173 \pm 0.259$ as determined in Ref. [30].

At $s = 0$ and setting the widths $\Gamma_{R_i} = 0$, with the constraints $G_E = 1$ and $G_M = \mu_{\Lambda_c^+} = 0.24\,\hat{\mu}_N$, the coefficients f_1 and f_2 in Eqs. (10) and (11) are obtained as

$$f_1 = 1 - \beta_1 - \beta_2 - \beta_3 - \beta_4, \tag{14}$$

$$f_2 = \mu_{\Lambda_c^+} - 1 - \alpha_2 - \alpha_3 - \alpha_4, \tag{15}$$

with $\beta_1 = 1.883 \pm 0.484$, $\beta_2 = -1.101 \pm 0.302$, $\beta_3 = -0.439 \pm 0.194$, $\beta_4 = -0.141 \pm 0.097$, and $\alpha_2 = 1.089 \pm 0.297$, $\alpha_3 = 0.438 \pm 0.192$, $\alpha_4 = 0.133 \pm 0.096$ the model parameters, which are fitted to the experimental data on the total cross sections, the ratio $|G_E/G_M|$ and G_M about the $e^+e^- \to \Lambda_c^+\bar{\Lambda}_c^-$ reaction.

III. SPIN POLARIZATION OF THE PRODUCED Λ_c^+ IN THE PROCESS OF $e^+e^- \to \Lambda_c^+\bar{\Lambda}_c^-$

In the time-like region, G_E and G_M are complex. The relative phase $\Delta\Phi$ between G_E and G_M is an observable

---

1) Here after, G_E and G_M stand for the electric and magnetic form factors of Λ_c^+.

physical quantity,

$$G_E/G_M = \mathrm{e}^{i\Delta\Phi}|G_E/G_M|. \tag{16}$$

Actually, $\Delta\Phi$ can be extracted experimentally from the spin polarization of the final Λ_c^+ in the reaction $e^+e^- \to \Lambda_c^+\bar{\Lambda}_c^-$. However, it is experimentally difficult to measure the spin polarization of baryons directly. The unexpected observation of spin polarization in $e^+e^- \to J/\psi \to \Lambda\bar{\Lambda}$ by the BESIII Collaboration [41] has opened new perspectives for such studies [18, 42−46].

Usually, the spin direction of Λ_c^+ is reconstructed by the final particle angular distribution of the Λ_c^+ weak decays, for example, $\Lambda_c^+ \to \Lambda + \pi^+$. Taking into account the final Λ_c^+ and $\bar{\Lambda}_c^-$ weak decays, the whole process as $e^+e^- \to \Lambda_c^+(\to \Lambda + \pi^+)\bar{\Lambda}_c^-(\to \bar{\Lambda} + \pi^-)$, its differential distribution can be expressed as [47, 48]

$$\begin{aligned}
\mathcal{W}(\xi) =\,& 1 + \alpha\mathcal{T}_5(\xi) + \alpha_{\Lambda_c^+}\alpha_{\bar{\Lambda}_c^-} \\
& \left[\mathcal{T}_1(\xi) + \sqrt{1-\alpha^2}\cos(\Delta\Phi)\mathcal{T}_2(\xi) + \alpha\mathcal{T}_6(\xi)\right] \\
& + \sqrt{1-\alpha^2}\sin(\Delta\Phi)[\alpha_{\Lambda_c^+}\mathcal{T}_3(\xi) + \alpha_{\bar{\Lambda}_c^-}\mathcal{T}_4(\xi)],
\end{aligned} \tag{17}$$

where $\xi = (\theta, \Omega_\Lambda, \Omega_{\bar{\Lambda}})$, and $\Omega_\Lambda, \Omega_{\bar{\Lambda}}$, is the momentum direction of the baryon Λ and $\bar{\Lambda}$ in the rest frame of Λ_c^+ and $\bar{\Lambda}_c^-$, respectively. Here, $\alpha_{\Lambda_c^+}$ is the decay asymmetry parameter for the $\Lambda_c^+ \to \Lambda + \pi^+$ decay, and $\alpha_{\bar{\Lambda}_c^-}$ for the $\bar{\Lambda}_c^- \to \bar{\Lambda} + \pi^-$. [1] In addition, these angular functions $\mathcal{T}_i\,(i = 1, 2, \cdots, 6)$ are given as follows:

$$\mathcal{T}_1(\xi) = \sin^2\theta\sin\theta_1\sin\theta_2\cos\phi_1\cos\phi_2 + \cos^2\theta\cos\theta_1\cos\theta_2,$$

$$\mathcal{T}_2(\xi) = \sin\theta\cos\theta(\cos\theta_2\sin\theta_1\cos\phi_1 + \cos\theta_1\sin\theta_2\cos\phi_2),$$

$$\mathcal{T}_3(\xi) = \sin\theta\cos\theta\sin\theta_1\sin\phi_1,$$

$$\mathcal{T}_4(\xi) = \sin\theta\cos\theta\sin\theta_2\sin\phi_2,$$

$$\mathcal{T}_5(\xi) = \cos^2\theta,$$

$$\mathcal{T}_6(\xi) = \cos\theta_1\cos\theta_2 - \sin^2\theta\sin\theta_1\sin\theta_2\sin\phi_1\sin\phi_2,$$

where $(\theta_1, \phi_1) = \Omega_\Lambda$, $(\theta_2, \phi_2) = \Omega_{\bar{\Lambda}}$. Note that the coordinate system is defined as follows: the z axis direction is along the momentum $\vec{p}$ of the emitted baryon Λ_c^+, and the y axis is perpendicular to the scattering plane along the direction $\vec{p} \times \vec{k}$, with $\vec{k}$ being the electron momentum, and the x axis is determined by the right-hand coordinate system, as presented in Fig. 1.

The term $1 + \alpha\mathcal{T}_5(\xi)$ in Eq. (17) is spin-independent, corresponding to the differential cross section angular distribution in Eq. (6). The second term multiplied by

$\alpha_{\Lambda_c^+}\alpha_{\bar{\Lambda}_c^-}$ represents the spin entanglement of Λ_c^+ and $\bar{\Lambda}_c^-$, while the last term stands for the spin polarization of the charmed baryon Λ_c^+ along the y axis. High statistic data samples close to the threshold for the $e^+e^- \to \Lambda_c^+\bar{\Lambda}_c^-$ reaction enabled studies of the angular distributions of Λ_c^+ in the e^+e^- center-of-mass system.

Experimentally, the information about spin polarization of charmed baryon Λ_c^+ in the joint reaction $e^+e^- \to \Lambda_c^+(\to \Lambda + \pi^+)\bar{\Lambda}_c^-(\to \bar{\Lambda} + \pi^-)$ at a certain energy $\sqrt{s}$ is mainly obtained by measuring the following angular distribution [16, 41, 49],

$$M(\cos\theta) = \frac{\alpha_{\Lambda_c^+} - \alpha_{\bar{\Lambda}_c^-}}{3 + \alpha}\sqrt{1-\alpha^2}\sin(\Delta\Phi)\sin\theta\cos\theta. \tag{18}$$

One can see that the $M(\cos\theta)$ will vanish at $\alpha = \pm 1$ or the relative phase $\Delta\Phi = 0$, otherwise, it reaches its maximum value at $\theta = \pi/4$ and vanishes at $\theta = 0$, $\pi/2$, and π. In general, in the time-like region, G_E and G_M are complex, thus $\Delta\Phi$ is not zero and α cannot reach ± 1, which indicates that the produced Λ_c^+ is polarized, even though the initial states e^+ and e^- are both unpolarized. The spin polarization of Λ_c^+ is directed along the normal to the $e^-e^+ \to \Lambda_c^+\bar{\Lambda}_c^-$ scattering plane, which is defined as $\vec{p} \times \vec{k}$. It is worth mentioning that if the y axis direction is defined by $\vec{k} \times \vec{p}$, there will be an additional minus in the angular distribution function Eq. (17), *i.e.*, replacing $\sin\theta$ with $-\sin\theta$.

IV.　NUMERICAL RESULTS AND DISCUSSIONS

The Driac and Pauli form factors $F_1(q^2)$ and $F_2(q^2)$ of the Λ_c^+ were constructed within the VMD model, in which four charmonium-like states were included, called $\psi(4500)$, $\psi(4660)$, $\psi(4790)$, and $\psi(4900)$. Then one can easily obtain the electromagnetic form factors of $G_E(q^2)$ and $G_M(q^2)$, and also the experimental observables. The model parameters are fixed by fitting them to the experimental data. By taking into account these vector excited states, the flat behavior of the total cross section from the threshold to $\sqrt{s} = 4.67$ GeV for the process $e^+e^- \to \Lambda_c^+\bar{\Lambda}_c^-$ [30] is successfully explained. Here, we present the detailed structure of the cross section near the reaction threshold, as shown in Fig. 2 by the blue solid line, where the quantity E is defined as $E \equiv \sqrt{s} - 2M_{\Lambda_c^+}$. One can see that the theoretical results are in agreement with the experimental data taken from the BESIII Collaboration [23], and the flat behavior of the total cross sections can be well reproduced. Moreover, it is found that the obtained value of the total cross section at the reaction threshold ($E = 0$) is about 193 nb, and $G_E(E = 0) = G_M(E = 0) = 0.92 - 0.71i$.

---

1) If CP is conserved in the charge conjugate decay, it will lead to $\alpha_{\Lambda_c^+} = -\alpha_{\bar{\Lambda}_c^-}$. Here, we take CP is conserved. The distribution function $\mathcal{W}(\xi)$ can be used to extract separately Λ_c^+ and $\bar{\Lambda}_c^-$ decay asymmetry parameters, and thus allowing to a direct test of CP violation in the hyperon weak decays.
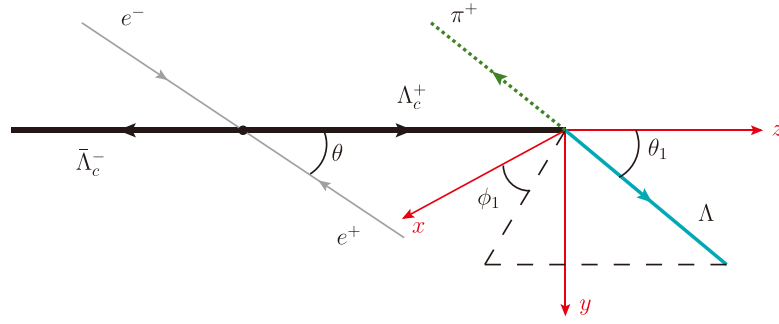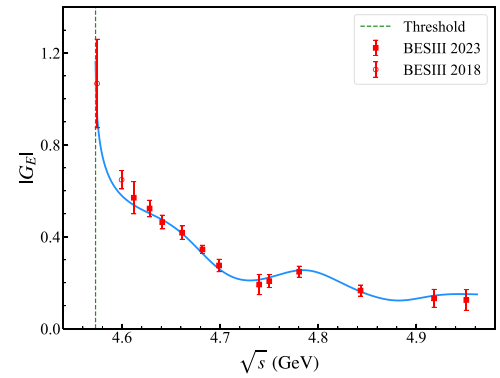
Fig. 1. (color online) The definition of the coordinate system in the reaction $e^+e^- \to \Lambda_c^+(\to \Lambda + \pi^+)\bar{\Lambda}_c^-(\to \bar{\Lambda} + \pi^-)$, where the decay of $\bar{\Lambda}_c^-$ to $\bar{\Lambda}\pi^-$ is not shown for simplicity. The solid angle $\Omega_\Lambda = (\theta_1, \phi_1)$ of Λ is defined in the center of the mass frame of Λ_c^+, and $\Omega_{\bar{\Lambda}} = (\theta_2, \phi_2)$ in $\bar{\Lambda}_c^-$ with the same coordinate system.
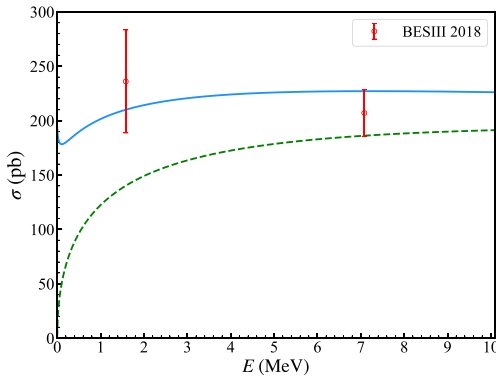
Fig. 2. (color online) The obtained total cross sections of the $e^+e^- \to \Lambda^+\bar{\Lambda}_c^-$ reaction as a function of the excess energy E comparison with experimental data taken from the BESIII Collaboration [23]. The blue solid line represents the theoretical results, which include the Sommerfeld–Gamow factor C, and the green dashed line excludes factor C.


Fig. 3. (color online) The obtained electric form factor $|G_E|$ compared with experimental data taken from Refs. [23, 24]. The green vertical dashed curves represent the $e^+e^- \to \Lambda_c^+\bar{\Lambda}_c^-$ kinematic reaction threshold.

To see the importance of factor C, we also plot the numerical results without including factor C in Fig. 2 by the green dashed line. One can see that factor C affects only the energy region very close to the reaction threshold [26]. Moreover, its affect decreases very quickly as the reaction energy grows. For energies above a few MeV of the reaction threshold, the impact of this Sommerfeld–Gamow factor is not very important. However, it does provide a nonzero cross section at the reaction threshold.

Because the total cross sections of the $e^+e^- \to \Lambda_c^+\bar{\Lambda}_c^-$ reaction can be measured at the reaction threshold, it is expected that more experimental measurements can be done to test our model calculations shown in Fig. 2. In fact, the BESIII detector has collected scan data at fourteen c.m. energies from the threshold to 4.95 GeV with relatively large statistics [33, 45]. Thus, it is possible that a high-precision production cross-section line shape of the $e^+e^- \to \Lambda_c^+\bar{\Lambda}_c^-$ reaction will be produced soon. These future experimental data will serve as crucial inputs for theoretical calculations concerning different production

mechanisms of Λ_c^+.

Next, in Fig. 3, the obtained modulus of the electric form factor $G_E(q^2)$ as a function of $\sqrt{s}$ are shown. One can see that the model can well describe the experimental data. In particular, the data point very close to the kinematic threshold can also be reproduced. On the other hand, there is a sizable bump structure around $\sqrt{s} = 4.78$ GeV in the line shape of $|G_E(q^2)|$, which is attributed to the charmonium-like state $\psi(4790)$ [32]. Further studies on this state on both the experimental and theoretical sides are most welcome [50].

The theoretical results for the angular distribution parameter α are presented in Fig. 4, and compared with the experimental data taken from the BESIII Collaboration [23, 24]. One can see that our theoretical results are in agreement with the experimental data especially in the c.m. energies from 4.64 to 4.90 GeV. Still, close to the reaction threshold, the theoretical results do not match the experimental values so well. However, more precise data around the reaction threshold are also needed. On the other hand, to improve the theoretical calculations near the reaction threshold, new $\Lambda_c^+\bar{\Lambda}_c^-$ bound states [51] might need to be introduced.
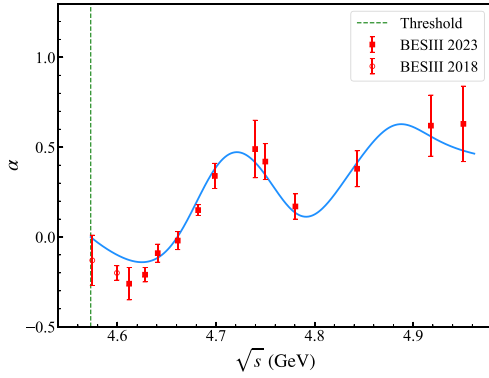
Fig. 4. (color online) As in Fig. 3, but for the theoretical results about the angular distribution parameter α compared with the experimental data from the BESIII Collaboration [23, 24].

As shown in Fig. 4, the line shape of α shows an oscillatory increasing behavior, which is a natural result according to Eq. (8), because the ratio of $|G_E/G_M|$ has a damped oscillation [30]. This so-called oscillating behavior is because of the production of the vector excited states. In addition to these studies on the EMFFs for the light baryons in Refs. [52−65], it is concluded that the non-monotonic structures observed in the line shape of the $e^+e^- \to B\bar{B}$ total cross sections can be naturally explained by including the contributions from the excited vectors within the vector meson dominance model.

In addition, with the obtained electromagnetic form factors or the parameter α, the differential cross sections of the $e^+e^- \to \Lambda_c^+\bar{\Lambda}_c^-$ reaction at $E = 5$, 50, 100, and 150

MeV can be easily calculated and the theoretical results are shown in Fig. 5. On the experimental side, the parameter α and the relative phase angle $\Delta\Phi$ between the electric and magnetic form factors of Λ_c^+ can be extracted from the differential cross sections of the $e^+e^- \to \Lambda^+\bar{\Lambda}_c^-$ reaction. Again, more experimental measurements about the differential cross sections from the experimental side are needed to test the theoretical calculations here and determine the individual electromagnetic form factors of Λ_c^+.

The obtained relative phase $\Delta\Phi$ between the electric G_E and magnetic G_M form factors are shown in Fig. 6. At the reaction threshold $E = 0$, the relative phase $\Delta\Phi$ equals zero because G_E is exactly equal to G_M according to Eqs. (4) and (5). As the energy E increases, the relative phase increases and remains constant at about 60° around $E = 120$ MeV. It is worth mentioning that it is difficult to get the relative phase $\Delta\Phi$ because the experimental cross sections depend on the modulus of G_E and G_M. To get this phase, one needs to measure the angular distributions of the $e^+e^- \to \Lambda_c^+\bar{\Lambda}_c^-$ reaction. In fact, the relative phase $\Delta\Phi$ could be measured from the spin angular distribution of the baryon, which was usually reconstructed from their weak decays. Meanwhile, the baryon spin polarization is self-analyzed in their weak decays.

Following Ref. [47] and according to the obtained form factors F_1 and F_2 within the VMD model, we can obtain the scattering amplitude of the $e^+e^- \to \Lambda_c^+\bar{\Lambda}_c^-$ reaction, from which we can study the spin polarization of Λ_c^+. With Eq. (18), where the details about the spin polar-
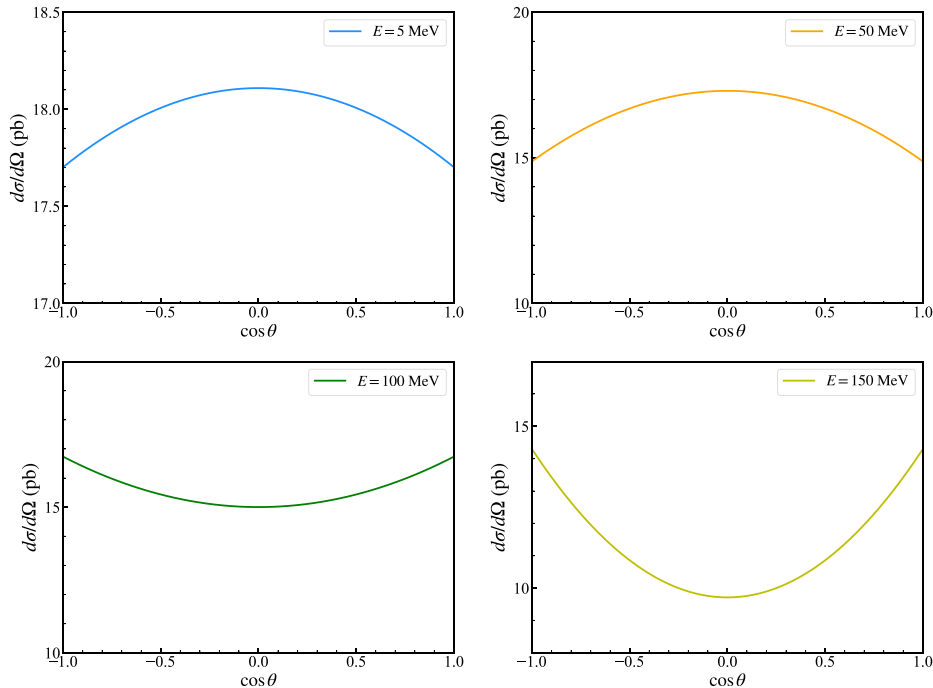
Fig. 5. (color online) The obtained differential cross sections of the process $e^+e^- \to \Lambda^+\bar{\Lambda}_c^-$ at excess energy $E = 5$, 50, 100, and 150 MeV.
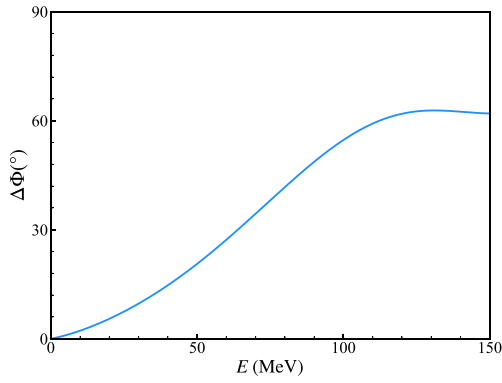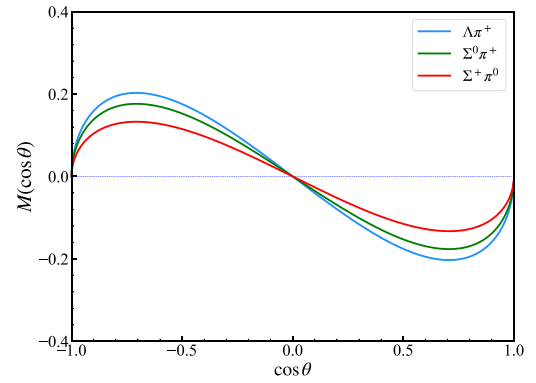
Fig. 6. (color online) The obtained relative phase $\Delta\Phi$ between G_E and G_M as a function of E.

Fig. 7. (color online) The obtained moments $M(\cos\theta)$ at $\sqrt{s} = 4.7$ GeV. The blue line represents the result of the decay of the final state Λ_c^+ to $\Lambda\pi^+$, the green line represents $\Lambda_c^+ \to \Sigma^0\pi^+$ and the red line represents $\Lambda_c^+ \to \Sigma^+\pi^0$, while the decay of $\bar{\Lambda}_c^-$ is the charge conjugation of Λ_c^+, respectively.

ization of Λ_c^+ along the y axis are given for the case of $\Lambda_c^+ \to \Lambda\pi^+$, the distributions of $M(\cos\theta)$ at $\sqrt{s} = 4.7$ GeV (*i.e.*, $E = 125$ MeV) are calculated. Because, near this energy point, it possesses a considerably larger relative phase, to such an extent that a more remarkable polarization can be experimentally observed. Furthermore, we have also calculated $M(\cos\theta)$ for the cases of $\Lambda_c^+ \to \Sigma^0\pi^+$ or $\Lambda_c^+ \to \Sigma^+\pi^0$. These three decay modes have larger decay branching ratios compared to other channels [66], and the decay asymmetry parameter $\alpha_{\Lambda_c^+}$ in the three final states $\Lambda\pi^+$, $\Sigma^0\pi^+$, and $\Sigma^+\pi^0$ are -0.84 ± 0.09, -0.73 ± 0.18, and -0.55 ± 0.11, respectively. In Fig. 7, we show our numerical results concerning the $M(\cos\theta)$ in the three decay channels at c.m. energies $\sqrt{s} = 4.7$ GeV. The blue line represents $\Lambda_c^+ \to \Lambda\pi^+$, the green line represents the $\Lambda_c^+ \to \Sigma^0\pi^+$, and the red line represents the $\Lambda_c^+ \to \Sigma^+\pi^0$. It is expected that the theoretical results for the $M(\cos\theta)$ can be measured by the BESIII Collaboration and Belle Collaboration in future experiments or at the planned super tau charm facility [67]. Regardless, it is worth anticipating that more experimental information will be available in the near future to greatly improve the knowledge about the production mechanism of the charmed baryon Λ_c^+ in the process of $e^+e^- \to \Lambda_c^+\bar{\Lambda}_c^-$.

V. SUMMARY

In summary, we investigated the electromagnetic form factors of the lightest charmed baryon Λ_c^+ and the total cross sections of the $e^+e^- \to \Lambda_c^+\bar{\Lambda}_c^-$ near threshold based on the extended vector meson dominance model. Using parameterizations of the electromagnetic form factors G_E and G_M available, the angular distribution parameter α was also calculated, which is consistent with the experimental data from the BESIII Collaboration. Moreover, the modulus of electric form factor G_E and the relative phase $\Delta\Phi$ between G_E and G_M were presented. The relative phase is associated with the spin polarization of the produced baryon in the $e^+e^- \to \Lambda_c^+\bar{\Lambda}_c^-$ reaction. With the obtained relative phase and the parameter α, the moments $M(\cos\theta)$ are obtained in three Λ_c^+ decay channels, $\Lambda_c^+ \to \Lambda\pi^+$, $\Lambda_c^+ \to \Sigma^0\pi^+$ and $\Lambda_c^+ \to \Sigma^+\pi^0$. Because the channel $\Lambda_c^+ \to \Lambda\pi^+$ has a larger decay asymmetry parameter compared to the other two decay modes, it is more likely that significant phenomena will be observed in the process $e^+e^- \to \Lambda_c^+(\to \Lambda\pi^+)\bar{\Lambda}_c^-(\to \bar{\Lambda}\pi^-)$. It is expected that the theoretical results obtained here can be tested by future experiments, such as BESIII and Belle II.

Finally, we would like to stress that, thanks to the important role played by the excited charmonium states in the $e^+e^- \to \Lambda_c^+\bar{\Lambda}_c^-$ reaction, more precise experimental measurements for this reaction, such as Belle II, BESIII, and STCF, can be used to improve our knowledge of the properties of some charmonium states, which are at present poorly known. More experimental information will be available in the near future, which will greatly improve our knowledge of the production mechanism of the process $e^+e^- \to \Lambda_c^+\bar{\Lambda}_c^-$.

References

[1] A. Denig and G. Salme, Prog. Part. Nucl. Phys. **68**, 113 (2013)

[2] S. Pacetti, R. Baldini Ferroli, and E. Tomasi-Gustafsson, Phys. Rept. **550**, 1 (2015)

[3] V. Punjabi, C. F. Perdrisat, M. K. Jones *et al.*, Eur. Phys. J. A **51**, 79 (2015)

[4] I. M. Gough Eschrich *et al.* (SELEX Collaboration), Phys. Lett. B **522**, 233 (2001)

[5] O. Gayou *et al*. (Jefferson Lab Hall A Collaboration), Phys. Rev. Lett. **88**, 092301 (2002)

[6] M. K. Jones *et al*. (Jefferson Lab Hall A Collaboration), Phys. Rev. Lett. **84**, 1398 (2000)

[7] M. Ablikim *et al*. (BESIII Collaboration), Phys. Rev. D **97**, 032013 (2018)

[8] M. Ablikim *et al*. (BESIII Collaboration), Phys. Rev. Lett. **124**, 032002 (2020)

[9] M. Ablikim *et al*. (BESIII Collaboration), Phys. Lett. B **820**, 136557 (2021)

[10] M. Ablikim *et al*. (BESIII Collaboration), Phys. Rev. D **104**, L091104 (2021)

[11] M. Ablikim *et al*. (BESIII Collaboration), Phys. Lett. B **814**, 136110 (2021)

[12] X. Wang and G. Huang, Symmetry **14**, 65 (2022)

[13] M. Ablikim *et al*. (BESIII Collaboration), JHEP **11**, 228 (2023)

[14] M. Ablikim *et al*. (BESIII Collaboration), JHEP **05**, 022 (2024)

[15] E. A. Kuraev, E. Tomasi-Gustafsson, and A. Dbeyssi, Phys. Lett. B **712**, 240 (2012)

[16] M. Ablikim *et al*. (BESIII Collaboration), Phys. Rev. D **105**, L011101 (2022)

[17] M. Ablikim *et al*. (BESIII Collaboration), JHEP **10**, 081 (2023)

[18] M. Ablikim *et al*. (BESIII Collaboration), Phys. Rev. Lett. **133**, 101902 (2024)

[19] M. Ablikim *et al*. (BESIII Collaboration), Phys. Rev. D **106**, L091101 (2022)

[20] M. Ablikim *et al*. (BESIII Collaboration), Phys. Rev. D **108**, L011101 (2023)

[21] H. Liu, J. Zhang, and X. Wang, Symmetry **15**, 214 (2023)

[22] G. Pakhlova *et al*. (Belle Collaboration), Phys. Rev. Lett. **101**, 172001 (2008)

[23] M. Ablikim *et al*. (BESIII Collaboration), Phys. Rev. Lett. **120**, 132001 (2018)

[24] M. Ablikim *et al*. (BESIII Collaboration), Phys. Rev. Lett. **131**, 191901 (2023)

[25] L. Y. Dai, J. Haidenbauer, and U. G. Meißner, Phys. Rev. D **96**, 116001 (2017)

[26] Q. F. Cao, H. R. Qi, Y. F. Wang *et al*., Phys. Rev. D **100**, 054040 (2019)

[27] A. I. Milstein and S. G. Salnikov, Phys. Rev. D **105**, 074002 (2022)

[28] J. Wan, Y. Yang, and Z. Lu, Eur. Phys. J. Plus **136**, 949 (2021)

[29] D. Guo, Q.-H. Yang, and L. Y. Dai, Phys. Rev. D **109**, 114005 (2024)

[30] C. Chen, B. Yan, and J. J. Xie, Chin. Phys. Lett. **41**, 021302 (2024)

[31] M. Ablikim *et al*. (BESIII Collaboration), Phys. Rev. Lett. **131**, 211902 (2023)

[32] M. Ablikim *et al*. (BESIII Collaboration), Phys. Rev. Lett. **131**, 151903 (2023)

[33] M. Ablikim *et al*. (BESIII Collaboration), Chin. Phys. C **44**, 040001 (2020)

[34] G. Huang and R. B. Ferroli (BESIII Collaboration), Natl. Sci. Rev. **8**, nwab187 (2021)

[35] A. D. Sakharov, Zh. Eksp. Teor. Fiz. **18**, 631 (1948)

[36] J. P. Lees *et al*. (BaBar Collaboration), Phys. Rev. D **89**, 111103 (2014)

[37] E. van Beveren and G. Rupp, Chin. Phys. C **35**, 319 (2011)

[38] E. van Beveren and G. Rupp, Phys. Rev. D **80**, 074001 (2009)

[39] E. van Beveren, X. Liu, R. Coimbra *et al*., EPL **85**, 61002 (2009)

[40] S. M. Flatté, Phys. Lett. B **63**, 224 (1976)

[41] M. Ablikim *et al*. (BESIII Collaboration), Nature Phys. **15**, 631 (2019)

[42] E. Perotti, G. Fäldt, A. Kupsc *et al*., Phys. Rev. D **99**, 056008 (2019)

[43] M. Ablikim *et al*. (BESIII Collaboration), Phys. Rev. D **103**, L091101 (2021)

[44] M. Ablikim *et al*. (BESIII Collaboration), Phys. Rev. D **108**, L031106 (2023)

[45] K. Schönning, V. Batozskaya, P. Adlarson *et al*., Chin. Phys. C **47**, 052002 (2023)

[46] M. Ablikim *et al*. (BESIII Collaboration), arXiv: 2408.03205

[47] G. Fäldt and A. Kupsc, Phys. Lett. B **772**, 16 (2017)

[48] X. Cao, Y. T. Liang, and R. G. Ping, Phys. Rev. D **110**, 014035 (2024)

[49] M. Ablikim *et al*. (BESIII Collaboration), Phys. Rev. Lett. **125**, 052004 (2020)

[50] W. Wang, X. Zhou, R. B. Ferroli *et al*., Symmetry **14**, 5 (2022)

[51] X. K. Dong, F. K. Guo, and B. S. Zou, Progr. Phys. **41**, 65 (2021)

[52] Y. H. Lin, H. W. Hammer, and U. G. Meißner, Phys. Rev. Lett. **128**, 052002 (2022)

[53] X. Cao, J. P. Dai, and H. Lenske, Phys. Rev. D **105**, L071503 (2022)

[54] B. Yan, C. Chen, X. Li, and J. J. Xie, Phys. Rev. D **109**, 036033 (2024)

[55] R. Q. Qian, Z. W. Liu, X. Cao *et al*., Phys. Rev. D **107**, L091502 (2023)

[56] S. Pacetti, R. Baldini Ferroli, A. Bianconi *et al*., Science Bulletin **67**, 557 (2022)

[57] J. P. Dai, X. Cao, and H. Lenske, Phys. Lett. B **846**, 138192 (2023)

[58] Y. Yang, D. Y. Chen, and Z. Lu, Phys. Rev. D **100**, 073007 (2019)

[59] Z. Y. Li, A. X. Dai, and J. J. Xie, Chin. Phys. Lett. **39**, 011201 (2022)

[60] Z. Y. Li and J. J. Xie, Commun. Theor. Phys. **73**, 055201 (2021)

[61] A. X. Dai, Z. Y. Li, L. Chang *et al*., Chin. Phys. C **46**, 073104 (2022)

[62] X. Cao, J. P. Dai, and Y. P. Xie, Phys. Rev. D **98**, 094006 (2018)

[63] B. Yan, C. Chen, and J. J. Xie, Phys. Rev. D **107**, 076008 (2023)

[64] L. Liu and C. S. Fischer, Eur. Phys. J. A **60**, 84 (2024)

[65] J. Haidenbauer, U. G. Meißner, and L. Y. Dai, Phys. Rev. D **103**, 014028 (2021)

[66] R. L. Workman *et al*. (Particle Data Group), Prog. Theor. Exp. Phys. **2022**, 083C01 (2022)

[67] F. K. Guo, H. Peng, J. J. Xie *et al*., arXiv: 2203.07141